Drought impacts on tree carbon sequestration and water use – evidence from intra-annual tree-ring characteristics

Elisabet Martínez-Sancho[1*], Kerstin Treydte[1], Marco M. Lehmann[1], Andreas Rigling[1,2], and Patrick Fonti[1]

[1]Research Unit Forest Dynamics, Swiss Federal Institute for Forest Snow and Landscape Research WSL, Zürcherstrasse 111, 8903 Birmensdorf, Switzerland
[2]Institute of Terrestrial Ecosystems, Swiss Federal Institute of Technology ETH, Universitaetsstrasse 16, 8092 Zurich, Switzerland

ORCIDs:
Elisabet Martínez-Sancho: 0000-0003-4413-6818
Kerstin Treydte: 0000-0001-8399-6517
Marco M. Lehman: 0000-0003-2962-3351
Andreas Rigling: 0000-0003-1944-4042
Patrick Fonti: 0000-0002-7070-3292

*Corresponding author: elisabet.martinez@wsl.ch

Received: *23 February 2022*
Accepted: *4 May 2022*

SUMMARY

- The impact of climate extremes on forest ecosystems is poorly understood but important for predicting carbon and water cycle feedbacks to climate. Some knowledge gaps still remain regarding how drought-related adjustments in intra-annual tree-ring characteristics directly impact tree carbon and water use.
- In this, study we quantified the impact of an extreme summer drought on the water-use efficiency and carbon sequestration of four mature Norway spruce trees. We used detailed observations of wood formation (xylogenesis) and intra-annual tree-ring properties (quantitative wood anatomy and stable carbon isotopes) combined with physiological water-stress monitoring.
- During 41 days of tree water deficit, we observed an increase in ^{13}C but a reduction in cell enlargement and wall thickening processes, which impacted the anatomical characteristics. These adjustments diminished carbon sequestration by 67% despite an 11% increase in

water-use efficiency during drought. However, with the resumption of a positive hydric state in the stem, we observed a fast recovery of cell formation rates based on the accumulated assimilates produced during drought.

- Our findings enhance our understanding of carbon and water fluxes between the atmosphere and forest ecosystems, providing observational evidence on the tree intra-annual carbon sequestration and water-use efficiency dynamics to improve future generations of vegetation models.

KEYWORDS

carbon sequestration, extreme drought, intrinsic water-use efficiency, physiological drought, point dendrometer, quantitative wood anatomy, stable carbon isotopes, xylogenesis

INTRODUCTION

Understanding the response of forest ecosystems to drought is increasingly important to better assess the magnitude and impacts of a warming climate (Werner *et al.*, 2022). By regulating evaporative cooling (Bala *et al.*, 2007) and sequestrating atmospheric carbon (Bonan, 2008), forests indeed play a major role in the global carbon and water cycles (Betts *et al.*, 2007; Friedlingstein *et al.*, 2020). However, the contribution of forests to mitigating climate change remains uncertain (Reichstein *et al.*, 2013; Friedlingstein *et al.*, 2014) because forest ecosystems themselves are also vulnerable to climate warming, and current dynamic global vegetation models (DGVMs) still need to be refined regarding some processes, such as those related to secondary growth (Zuidema *et al.*, 2018).

Tree physiology intimately connects the carbon and water cycles via two distinct processes. At the stomatal level carbon is absorbed from the atmosphere in exchange for water, while assimilated carbon is fixed in wood at the cambial level during tree growth. During the process of carbon uptake in the stomata, trees unavoidably lose large amounts of water, contributing about 60% of the total annual evapotranspiration on average at the ecosystem level (Schlesinger & Jasechko, 2014). At the same time, through the process of wood formation, forests capture a substantial amount of anthropogenic carbon emissions (Pan *et al.*, 2011; Harris *et al.*, 2021; Xu *et al.*, 2021) and serve as one of the main terrestrial carbon reservoirs. However, one of the main reasons for the uncertainty concerning the role of trees in mitigating climate change is the lack of empirical data with a high temporal resolution. This kind of data is needed to improve the understanding of processes such as growth (Lovenduski & Bonan, 2017; Babst *et al.*, 2020), and consequently it will help us to appropriately represent these processes in current DGVMs (Zuidema *et al.*, 2018; Friend *et al.*, 2019). For instance, most DGVMs still estimate growth from the difference between photosynthesis and plant respiration, without an explicit representation of growth processes themselves (Friend *et al.*, 2019). However, there is clear evidence that the environmental sensitivity differs between photosynthesis (source) and secondary growth (sink) (Fatichi *et al.*, 2013; Körner, 2015). Recent efforts using tree rings to benchmark the impact of extreme drought events on forest productivity (Anderegg *et al.*, 2015; Trotsiuk *et al.*, 2020) not only demonstrated the inability of current models to account for the pervasive impact on the global carbon cycle, but also emphasized the need for a more mechanistic inclusion in climate-vegetation models of the full cascade of causes–effects and legacies that influence tree growth performance. A tree-centered approach, i.e., the study of individual trees as a main source of information for understanding variability in growth (Sass-Klaassen *et al.*, 2016), could contribute to a more in-depth understanding of causal processes occurring within trees in response to environmental change.

Under limited water conditions, like those forecasted in future climate scenarios (IPCC, 2021), tree physiology is strongly disturbed, which indirectly affects the mitigation capacity of forest ecosystems to sequestrate carbon. For example, based on the measurement of fluxes at the ecosystem level, the 2003 summer drought that occurred in central Europe caused a 30% reduction in net primary productivity, temporarily turning some terrestrial ecosystems into a net carbon source (Ciais *et al.*, 2005). However, due to the high sensitivity of cell division and enlargement to both cell turgor and sugar availability (Fatichi *et al.*, 2013; Körner, 2015; Cabon *et al.*, 2020b; Peters *et al.*, 2020), wood formation could be constrained while photosynthesis still occurs. Due to the complexity of the processes involved in wood formation – which is characterized by cells undergoing several climate-sensitive phases until they become functional (Rathgeber *et al.*, 2016) – a drought event can also have several repercussions on the anatomical structure of the forming wood (e.g., Eilmann *et al.*, 2011; Fonti *et al.*, 2013). This could imply that the carbon fixed in wood does not represent the net amount between carbon absorbed at the leaf level and carbon respired; consequently, the impact of extreme droughts on tree carbon budgets could be systematically underestimated.

Water-use efficiency (iWUE) is the associated ratio of carbon uptake per unit of water loss (Farquhar *et al.*, 1982), and it can be measured using stable carbon isotope ratios (i.e., $\delta^{13}C$). The anthropogenic atmospheric CO_2 fertilization partially counteracts water dependencies by increasing leaf-scale photosynthesis and iWUE, implying that trees need less water to absorb the same amount of carbon. Indeed, during the twentieth century, broadleaf and coniferous trees across Europe displayed an increase in iWUE of 14±10% and 22±6%, respectively (Frank *et al.*, 2015), fostering a positive terrestrial carbon sink (Walker *et al.*, 2020). However, increases in iWUE are also related to the active role of trees in reducing stomatal conductance as a strategy to cope with water limitations (see references in Shestakova & Martínez-Sancho, 2021). Although several studies have demonstrated that this effect occurs in dry years (Battipaglia *et al.*, 2014; Olano *et al.*, 2014), still little is known about how iWUE varies around a drought event and its recovery dynamics.

Despite potential mismatches based on meteorological quantifications on the intensity of a drought event (see e.g., Slette *et al.*, 2019; Zang *et al.*, 2020), the above-mentioned physiological processes and their climatic thresholds also depend on the timing, duration and strength of a drought event. Further, a single drought event might impact individual trees differently according to their site-specific conditions (e.g., soil depth, topography), species characteristics (e.g., rooting system, tree height, tree age, drought adaptations), and physiological status (Anderegg *et al.*, 2013a; Bennett *et al.*, 2019). The severity of a given water stress as it is experienced by an individual tree is indeed a main factor determining stomatal regulation (Klein, 2014), as well as the processes of cell division, enlargement and wall thickening (Cuny *et al.*, 2014; Rossi *et al.*,

2014). This ultimately affects the amount of water transpired and the carbon sink capacity. The different environmental sensitivities of wood formation and photosynthesis, including their potential interactions, together with potential iWUE adjustments and a discrepancy between meteorological drought and physiological water stress, might partly explain the observed discrepancies between DGVMs and tree-ring observations (Babst *et al.*, 2013; Klesse *et al.*, 2018). In this study, we used highly-resolved data on xylogenesis, quantitative wood anatomical parameters, and stable carbon isotopes to assess the impact of an extreme summer drought on the resilience of the intra-annual carbon sequestration and water-use dynamics of mature Norway spruce trees growing in a natural subalpine forest. We hypothesized that (i) growth processes during drought, including cell formation and anatomical characteristics, would directly impact the ability of trees to sequestrate carbon; (ii) tree water losses during drought would be dramatically reduced as a consequence of fast physiological adjustments; and (iii) resilience patterns would be distinct for anatomical parameters and stable carbon isotope ratios due to differences in source and sink dynamics during and after drought.

MATERIALS AND METHODS

Study site and selected growing seasons

We conducted our study at the Lötschental tree growth monitoring transect (https://www.wsl.ch/loetschental-monitoring), where most of the required environmental and growth-related data were available. We selected a drought-exposed site located at the valley bottom (46° 23' 40'' N, 7° 45' 35'' E), at an elevation of 1,360 m a.s.l. We analyzed four adult individuals of Norway spruce (*Picea abies* (L.) Karst.) (Table S1), which is a central European species that has been classified as drought sensitive (Lebourgeois *et al.*, 2010).

We selected two years with distinctly different meteorological conditions: 2014 as a "normal" year not significantly different from the climatic long-term mean, and 2015 as a year characterized by an extreme summer drought in Central Europe (Orth *et al.*, 2016). According to the April to September mean temperature and precipitation sum, the two selected growing seasons were within the 1961–2016 average (2014) and at its hot and dry margin (2015) (Fig. S1). The anomalies observed in 2015 corresponded to precipitation lower by almost two-thirds (24 vs. 60 mm) and temperature 4°C higher (18.2°C vs. 14.2°C) than the long-term July mean.

Monitoring environmental and physiological water stress

Highly-resolved environmental and tree physiological water stress data were used to track the intensity of drought over time. Site environmental measurements aggregated during daytime hours (06:00–22:00 h CET) included: maximum air temperature (T air, °C) and average relative

humidity (RH, %) at 2 m above ground (U23-002 HOBO Pro; Onset, Bourne, MA, USA), and average soil volumetric water content at 10 cm depth (SVWC, %; ECH_2O EC-5; METER Group, Pullman, WA, USA). Furthermore, vapor pressure deficit (VPD, kPa) was also calculated based on this data. Tree physiological water stress was quantified for the local vegetation using the normalized difference vegetation index (NDVI) and the tree water deficit (TWD) measured in the stem (Zweifel *et al.*, 2005). Specifically, the crown stress level was assessed using four-day composite NDVI values retrieved from the Moderate Resolution Imaging Spectroradiometer (MODIS/Terra) of 250 m resolution centered on the study site. Relative stem shrinkage caused by low water potentials during drought and measured as stem radius variation is commonly referred to as TWD, and it represents the physiological response of trees to changing climate conditions in terms of growth and water status (Zweifel *et al.*, 2005). When TWD lasts more than 24 hours, it means that the tree could not recover its water status during the night. Stem radius variations were measured at 1.3 m stem height with a sub-hourly resolution using high-precision point dendrometers (DR model, Ecomatik, Munich, Germany).

Timing of individual cell formation

To determine the period each individual wood cell spent in the differentiating phases of cell enlargement and wall thickening, weekly microcores were collected at about 1–1.5 m stem height using a Trephor increment puncher (Rossi *et al.*, 2006a) during two growing seasons (N= 244 samples). All samples were stored in 70% ethanol. Microcores were processed to obtain microsections that allow retrospective observations. The samples were first embedded in paraffin with a HistoCore PEARL tissue processor (Leica Biosystems, Nussloch, Germany) to stabilize the unlignified tissues. The microcores were then cut at a thickness of 7 µm using a rotary microtome (RM2245, Leica Biosystems). The obtained sections were then stained with a solution of Astra blue and Safranin and permanently mounted on glass slides for digital imaging in both bright and polarized light (Axio Scan.Z1, Zeiss, Jena, Germany). Observations were then performed along three radial files per sample by counting the number of cells in the cambial, enlargement, wall thickening and mature phases, according to Rossi *et al.* (2006b).

The changes in the number of cells in the cambium and in the consecutive phases of xylem differentiation throughout the growing season were analyzed by fitting generalized additive mixed models (GAMMs) assuming a quasi-Poisson distribution of residuals (Wood, 2006). GAMMs were fitted using the package *mgcv* in R (R Development Core Team, 2015). Diagnostic plots were checked for heteroscedasticity, non-normal distribution and autocorrelation of the residuals from all GAMMs and were corrected when required. Day of year (DOY) was the main predictor and tree ID was included as a random effect to account for non-independent data (i.e., repeated measures over time).

Kinetics, including the timing (date of initiation and cessation) and duration (number of days), of the phases (cambial, enlargement, wall thickening and mature phases) for each cell in each ring, were calculated in a way similar to the approach of Cuny *et al.* (2013) and Pérez-de-Lis *et al.* (2021) (see details in Notes S1 and Fig. S2). The outputs of cell kinetics of the two years (2014 and 2015) were compared with parametric *t*-tests. Afterwards, phase durations were combined with wood anatomical measurements to calculate rates of enlargement and wall thickening.

Cell anatomy and rates of cell formation

One 1-cm diameter increment core was collected at 1.3 m stem height in 2020 from each of the four trees included in the section above. Cell anatomical measurements of mature tracheids were performed from high-resolution images (2.26 μm/pixel) of 12-μm-thick transversal microsections processed following the same method as for the microcores. Microsections were obtained from one longitudinal half of the collected cores. Using the software ROXAS (von Arx & Carrer, 2014) we measured the transversal cell lumen area (CLA), cell-wall area (CWA), total cell area (CTA = CLA + CWA), cell radial wall thickness (CWTrad), cell radial lumen diameter (CLArad), and cell radial diameter (Crad = 2 × CWTrad + CLArad), and positional coordinates of each tracheid included in the annual rings from 2014 and 2015. The R package *Raptor* (Peters *et al.*, 2018) was then used to assign each tracheid to its radial file and to obtain an average value for each position. Afterwards, CTA, CWA, Crad and CLA were fitted with GAMMs to assess their dynamics across the ring width, with DOY as the main predictor and tree ID as a random effect. To calculate the daily rates of cell enlargement and wall thickening, we subsequently divided CTA and CWA of each cell by the corresponding time spent in the enlargement (dE) and cell wall thickening (dW) phases, as described in Cuny *et al.* (2013) (see Notes S1 and Fig. S2).

Stable carbon isotope measurements and iWUE calculations

Intrinsic water-use efficiency (iWUE) calculations were derived from high-resolution measurements of tree-ring $\delta^{13}C$. Samples for isotope analysis were prepared using tangential cuts from the second longitudinal half of the 1-cm diameter cores. The thickness of the tangential sections (60 μm in the earlywood and 40 μm in the latewood) were selected to account for tracheid size changes across the ring width. Cuts were performed with a rotary microtome (Leica RM2245) surrounded by two digital cameras to guide the orientation of the cuts and document their thickness. A total of 398 tangential samples were collected (~50 consecutive intra-annual samples per ring and tree). Subsequently, holocellulose was extracted from each wood sample (Boettger *et al.*, 2007), homogenized using an ultrasonic treatment (Laumer *et al.*, 2009), and freeze-dried, then inserted into tin capsules for combustion to CO_2 using a EURO Elemental Analyzer (EuroVector, Milan, Italy). Stable carbon isotope ratios were measured by isotope ratio

mass spectrometry (IRMS) using a Delta V Advantage IRMS (Thermo Fisher Scientific, Bremen, Germany) with a precision of 0.02‰ (derived from parallel measurements of reference material). Carbon isotope ratios were reported with the delta (δ) notation indicating the $^{13}C/^{12}C$ ratio of a sample relative to that of the international standard VPDB (Vienna Pee Dee Belemnite) expressed in per mil.

Using the $\delta^{13}C$ values of the cellulose samples of the microsections ($\delta^{13}C_S$), we calculated the discrimination against ^{13}C ($\Delta^{13}C$) during carbon diffusion and fixation by plants, the estimated leaf intercellular CO_2 concentration (C_i), and the iWUE following the formulas described in Notes S2. Afterwards, the $\delta^{13}C_S$, $\Delta^{13}C$, Ci and iWUE values were then fitted with GAMMs to assess their dynamics across the ring width. The position occupied by the tangential section was included as a predictor and tree ID as a random effect.

Space-for-time conversion of cell features

To align the cell anatomical features, their corresponding rate of development, and the iWUE measurements along the time axis, we translated the cell positions (analyzed as % of the ring width) into the corresponding time of cell formation (analyzed as DOY) using the calculated time of cell formation (see Notes S1 and Fig. S2; space-for-time conversion adapted from Pérez-de-Lis *et al.* 2021). Specifically, the outcomes of the GAMMs (anatomical features: cell area, cell wall area and cell lumen area; intra-annual $\delta^{13}C$-derived variables: $\delta^{13}C$, $D^{13}C$, C_i and iWUE) were analyzed accounting for their relative position in the ring width by using % of the ring width as a predictor. The space-for-time conversion could then be performed because we knew the exact position of the cell within the tree ring and could extract the time it spent in the enlargement and cell wall thickening phases from the time models. In the specific case of $\delta^{13}C$-derived variables, we used the timing of the cell wall thickening phase, as we assumed that the cell isotopic signature mainly represented the content of the secondary cell wall and the environmental drivers that contributed to its formation.

Calculations of tree-level daily carbon sequestration

The intra-annual cell anatomical assessments provided the basis to upscale tree daily aboveground woody biomass production (kg carbon) to the tree level. Following Cuny *et al.* (2015), the daily woody biomass production per tree was calculated based on the sum of the rates of wall deposition occurring in all cells growing during a given day. The upscaling to the tree level was performed by considering the number of radial cell files composing the tree ring and the tree allometry; and by accounting for the wall density and its carbon content (see detailed information in Notes S3). All statistical analyses were performed in the R environment version 4.1.2 (R

Development Core Team, 2015) and graphics were designed using the R package *ggplot2* (Wickham, 2009).

RESULTS

The 2015 summer drought at the study site

The 2015 summer drought was identified as a distinct anomaly from the long-term annual mean values of all considered climate variables, as well as from the 2014 growing season values (Figs. 1A, S1). For the period June to August, the year 2015 displayed an increase of 7.4 °C in maximum daytime temperatures, a decrease of 18.6% in average relative humidity, an increase of 0.8 kPa in average vapor pressure deficit, and a decrease of 7.3% in average soil water content in comparison to the same period in 2014 (Fig. 1). The extreme drought in 2015 clearly affected the local vegetation, which showed an NDVI reduction during the period 19 June to 6 August, compared with both the long-term average (Fig. S3) and the year 2014 (Fig. 1B). Moreover, dendrometer data indicated 41 consecutive days of tree stem shrinkage during 2015, from 19 June to 30 July, with the maximum amount of shrinkage occurring on 19 July (Figs. 1C, S4). This period will be referred to as the drought period throughout the results section.

Changes in kinetic cell formation

The analyses of the weekly collected microcores revealed that the extreme summer drought of 2015 strongly altered the kinetics of cell formation and, hence, the tree-ring formation. The drought was mirrored by a significant reduction in the number of cells in each phase of cell formation compared with the previous growing season (Fig. 2). Indeed, the decrease in the number of cells in the cambial phase (on average -31%) and wall thickening phase (-30%) was concomitant with the occurrence of the TWD, whereas its effects were visible earlier in the case of cells in the enlargement phase (-36%). Its phenology was, however, less affected, as the timing of the beginning of the cambial, enlargement, wall thickening and mature phases was rather similar in the two years (Fig. 2, Table 1). A similar final number of cells was produced in the two years. However, the kinetics of cell formation were different between years (Fig. S5). In 2014, the duration of the cell enlargement phase increased slightly from the first to the last tracheid (Fig. S5 A, C). This trend was even more evident for the duration of the cell wall thickening phase. In comparison to 2014, the phases of cell enlargement and wall thickening lasted longer during the 2015 drought period (Fig. S5 B, D). However, the cell enlargement phase was shorter compared with 2014 values for the cells formed after the 2015 drought (Fig. S5 B, D). Thus, the extreme summer drought influenced 60% of the 2015 ring by affecting at least one of the phases of cell development.

Changes in the rate of cell formation and anatomical characteristics

The total cell areas were significantly smaller in 2015 than in 2014 for the 45–75% ring portion (Fig. 3A). This portion of the ring was associated with cells that underwent the enlargement phase during the summer drought of 2015 (Fig. 3B). The pattern of the rate of cell enlargement also differed between years (Fig. 3C). Both rings showed an increase in the rate of enlargement in the first cells, and this rate was higher in 2015. Afterwards, during the 2015 summer drought, the rate of cell enlargement decreased by more than 50%. Surprisingly, the rate increased again after the cessation of the dry period, whereas it continuously decreased in 2014.

Further, cells located in the middle of the 2015 ring (25–85%) also had significantly smaller wall areas than those from the same portion of the 2014 ring, despite the fact that cells located in the first 25% of the 2015 ring had larger wall areas than those from 2014 (Fig 3D). The cells with a reduced wall area in the 2015 ring completed the wall thickening phase during the summer drought (Fig. 3E). The rate of cell wall thickening was higher in 2015 than in 2014 at the beginning of the growing season (Fig. 3F). However, this situation was reversed as soon as the summer drought started, i.e., rates of wall thickening dropped in mid-July 2015, but they reached their maximum values at about the same time in 2014. The rates of wall thickening almost reached pre-drought levels after the cessation of the summer drought, and showed similar values to those of 2014 at the end of the growing season (Fig. 3F). Similarly, significant differences between years in cell lumen area were detected in the first 35–80% of the ring width (Fig. 3G), but these were not clearly associated with the period of wood formation (Fig. 3H). The observed changes in the anatomical characteristics of the cells formed during drought (Fig. 3) mean that the reduced rates of formation could not be compensated by increased phase durations (Fig. S6).

Variations in $\delta^{13}C$ and iWUE

The intra-annual tree-ring $\delta^{13}C$ variations were significantly different between the two years (Fig. 4, Fig. S7). The $\delta^{13}C$ values started at a slightly higher level in 2014 (-25.2‰) compared with in 2015 (-25.7‰). Despite an increasing trend during the first 20% of the ring in both years, $\delta^{13}C$ values then decreased steadily in 2014 but continued to increase towards a maximum (-24.0‰) at 55% of the ring in 2015. High $\delta^{13}C$ values in 2015 coincided with the timing of the drought (Fig. 4B), when many cells were in the wall thickening phase (40% of the ring). The $\delta^{13}C$ values in 2015 decreased again at the end of the summer drought but remained significantly higher than in 2014 for the rest of the ring.

Similarly, the $\delta^{13}C$-derived variations in $\Delta^{13}C$, Ci and iWUE differed between years. During 2014, we observed a decrease in $\Delta^{13}C$ and Ci from the beginning of the growing season to the end of June (Fig. 4C, D), which resulted in an increase in iWUE (from 93.03 to 97.13 μmol CO_2 mol

H_2O^{-1}; Fig 4E). Subsequently, the $\Delta^{13}C$ and Ci increased and iWUE decreased steadily until the end of the growing season. Although $\Delta^{13}C$ and Ci were higher at the beginning of 2015 compared with in 2014, we observed a decrease in both parameters during the summer drought. This resulted in an enhanced iWUE over a longer period in 2015 than in 2014 (maximum iWUE 107.8 and 97.4 µmol CO_2 mol H_2O^{-1} in 2014 and 2015, respectively, corresponding to an increase of 10.6%).

Impacts on tree-level daily carbon sequestration

The intra-annual dynamics of daily tree carbon sequestration through woody biomass production showed a strong fingerprint of the 2015 extreme drought. While daily woody biomass production showed a bell shape in the reference year 2014, reaching its maximum during the first weeks of July, the 2015 dry spell clearly negatively affected woody biomass production (Fig. 5). During the 41-day drought period, the average tree gained 67% less carbon (2.692 kg versus 4.033 kg) than in the 2014 reference period. We observed an earlier growth start and more favorable woody biomass production at the beginning of 2015 compared with 2014. Carbon sequestration resumed strongly after the drought, however, and reached even higher values than in 2014 (+23%), indicating an important compensating activity (Fig. 5). Notably, this effect resulted in an equivalent total amount of carbon being sequestered in woody biomass in the two years (7.261 kg in 2014 and 7.349 kg in 2015).

DISCUSSION

In this study, we quantified the impact of an extreme summer drought on Norway spruce water-use efficiency and carbon sequestration using a unique set of detailed retrospective observations of wood formation and intra-annual tree-ring properties (xylem cell anatomy and stable carbon isotopes) combined with measurements of physiological water stress. Our measurements of physiological stress clearly indicated that both the local ecosystem (via NDVI values) and the selected trees (via TWD) responded strongly to the meteorological extreme drought event in 2015. We observed imprints of drought on the cell kinetics, anatomical features and isotopic signatures of the formed cells, as a consequence of physiological adjustments to cope with water limitations. During the drought period, fewer cells were produced, cells were smaller with thicker cell walls, cells remained longer in the formation phases, and trees lost less water during gas exchange than during average growing seasons. Such physiological adjustments indirectly impacted the capacity of trees to sequester carbon and use water in the drought year 2015 compared with the reference year 2014. However, the different resilience patterns observed in the anatomical characteristics and stable carbon isotopes suggest that secondary growth might not be constrained by carbon availability.

The physiological responses triggered by water deficit

In our study, we made use of a physiological definition of drought based on a proxy for stem dehydration, i.e., tree water deficit (TWD; Zweifel *et al.*, 2005). This is a measure of stem radial shrinkage caused by water depletion from living tissues when transpiration exceeds water uptake (Dietrich *et al.*, 2018). This measure made it possible to precisely identify when and for how long the 2015 extreme summer drought impacted the water status of the studied trees, and this 41-day period matched surprisingly well with the period with altered growth processes. This period can still be considered moderate in length compared with, for instance, the 91 days of TWD observed at a low-elevation site (490 m a.s.l.) in southern Germany in the same year (Schäfer *et al.*, 2019).

Our observations of reduced xylem cell division and smaller cells formed under drought support the current understanding of the biophysical mechanisms underlying the rates cell enlargement. Cell division and enlargement are limited under water deficit (Génard *et al.*, 2001), as turgor is needed to expand the primary cell wall of the forming cells (Hsiao, 1973). Studies using mechanistic modelling have confirmed the major role of turgor in tracheid enlargement and size (Cabon *et al.*, 2020a; Peters *et al.*, 2020). These results are confirmed by observations in water-limited environments where long time-series of earlywood characteristics were found to correlate better with precipitation than with temperature (Martin-Benito *et al.*, 2013; Castagneri *et al.*, 2018). Our study also showed that cell wall thickening rates were reduced during the period of water deficit, consistent with findings from other studies (Olano *et al.*, 2014; Stangler *et al.*, 2021). Limited water availability during xylogenesis can influence the amount of non-structural carbohydrates (NSCs) available for use in cell wall thickening, as NSCs are instead required to counteract turgor loss by increasing osmotic potential (Deslauriers *et al.*, 2014). The previously described mechanism of compensating for reduced cell development rates by increasing phase duration also occurred in our trees (Cuny & Rathgeber, 2016; Cuny *et al.*, 2019). This alteration mitigates the impact of climatic conditions on the cell anatomical structure (Balducci *et al.*, 2016) and ensures xylem functionality and adequate tree growth (Lachenbruch & Mcculloh, 2014). However, the extended periods spent in both formation phases did not suffice to avoid altered anatomical characteristics. Overall, these anatomical responses to the extreme event of 2015 reduced the amount of carbon sequestrated in the stem during the summer drought: 67% less than in the same period of an average year.

It is also valuable to note that despite the relatively long water deficit of 41 days, we did not observe a complete cessation of the processes of cell division and enlargement, as has been previously documented in drier environments (Camarero *et al.*, 2010; Eilmann *et al.*, 2011). Our observations are in contrast to the zero-growth concept associated with dendrometer

measurements affirming that growth (defined as a permanent radial increment) cannot occur under stem shrinkage (Zweifel *et al.*, 2016). This minor conceptual incongruency might be due to a different definitions of growth (Hilty *et al.*, 2021, expansive vs. structural), which can have great relevance when assessing the effect of meteorological variables on cambial activity. Furthermore, the earlier start of the growing season in 2015 compared with 2014 is likely due to the warmer spring conditions that promote radial growth (Rossi *et al.*, 2008, Delpierre *et al.*, 2019, Huang *et al.*, 2020) and increased annual growth in mesic climates (e.g., Babst *et al.*, 2019, Anderson-Teixeira *et al.*,2021).

Our results showed that the period of tree water deficit also affected the carbon–water exchange of the studied trees, as indicated by an increase in $\delta^{13}C$ values during the extreme drought, which translated into lower $\Delta^{13}C$, lower Ci, and therefore higher iWUE. $\delta^{13}C$ ratios are highly influenced by changes in photosynthetic activity and/or in stomatal conductance, which are indeed strongly coupled (Farquhar *et al.*, 1989). Soil and atmospheric water deficits during the extreme drought period are more likely to lead to a closure of stomata than a reduction in photosynthetic rates, which would better explain the $\delta^{13}C$ increase (Battipaglia *et al.*, 2014). Indeed, stronger regulation of the stomata is necessary to reduce water loss by transpiration, causing a more parsimonious use of water for a given amount of assimilated carbon. An increase in iWUE is thus often interpreted as a reaction to drought to facilitate the maintenance of a positive carbon balance under dry conditions (Raven, 2002). We found that water deficit increased the seasonal maximum water-use efficiency by 10.6% in the dry compared with the normal growing season, in line with other studies of intra-annual $\delta^{13}C$ patterns under dry conditions (Sarris *et al.*, 2013; Battipaglia *et al.*, 2014). We cannot exclude post-photosynthetic fractionation processes due to the remobilization of reserves, which would partially decouple the isotopic signal of stem cellulose from the leaves (Gessler *et al.*, 2014; Bögelein *et al.*, 2019). Nonetheless, the tight match between TWD and increased $\delta^{13}C$ indicates an immediate and direct incorporation of the assimilates produced under dry conditions into the forming wood structure. Indeed, labelling experiments on mature coniferous trees have shown that the isotopic signal in the leaves can be transferred down the stem within few days (Gao *et al.*, 2021).

These physiological adjustments, i.e., reduced stomatal conductance and reduced cell and lumen area, increase the hydraulic resistance to water flow throughout the tree (Sviderskaya *et al.*, 2021), but at the same time they enhance the hydraulic safety against interruptions to sapflow due to cavitation and embolism (Hacke & Jansen, 2009; Bouche *et al.*, 2014). Both of these adjustments are therefore important for coping with decreasing water potentials under drought. Our findings are in agreement with results from physiological studies indicating an early physiological response to water limitations in Norway spruce (Lu *et al.*, 1995; Ditmarová *et al.*, 2009). Our observations demonstrate that water deficit does not always completely curtail wood

formation processes, but limits growth before a reduction in photosynthesis occurs. These responses, however, might have different impacts depending on the timing and severity of the drought with respect to the tree physiological and phenological status. For instance, a severe drought might induce dramatic hydraulic failures, causing leaf shedding with pervasive legacies (Anderegg *et al.*, 2015) and exposing declining trees to a higher risk of mortality (e.g., Timofeeva *et al.*, 2017; Camarero *et al.*, 2018). Additionally, whether the drought event occurs early or late in the season might have different impacts on tree-ring radial growth (Salomón *et al.*, 2022; Etzold *et al.*, 2022).

Post-drought recovery

Our findings indicated a rapid and strong recovery of cell enlargement and wall thickening rates after the drought event – a doubling of the minimum rates observed during the drought to reach almost the pre-drought levels – as soon as the drought period was over (TWD turned positive). Moreover, the observed rates were far above the levels observed for the reference year 2014. Although we did not observe an increase in cell production during the hydric resumption, this boost in activity nevertheless affected carbon sequestration at the cellular level in the post-drought period. Notably, the $\delta^{13}C$ values of these cells remained about 1‰ higher than in 2014. This difference was even higher for $\Delta^{13}C$, Ci and iWUE because we also accounted for seasonal atmospheric $\delta^{13}C$ variations in these calculations.

We interpret these results (i.e.; the drought-induced reduction and the subsequent post-drought boost in sink activity) as a direct consequence of changes in the interaction between the wood formation processes and carbon assimilate production. Despite a reduction in leaf physiological processes during drought conditions, assimilate production still continues with a higher isotopic signal, although incorporation into sinks is minimal (Tomasella *et al.,* 2017), due to the different climatic sensitivities of photosynthesis and growth (Fatichi *et al.*, 2013; Körner, 2015; Hagedorn *et al.*, 2016). Previous findings of an accumulation of non-structural carbohydrates under low water availability (Dietze *et al.*, 2014; Piper *et al.*, 2017) and reduced transfer to storage tissues (Rademacher *et al.*, 2021) support our results. After the resumption of an improved tree hydric status, the assimilates that accumulated during drought are readily available and rapidly incorporated into wood formation processes, which are no longer constrained by water limitation (Gessler *et al.*, 2020). Our results also suggest that carbon assimilates that have not yet been stored are the main driver of sink activity (Rademacher *et al.*, 2021), but only under favorable conditions for cambial activity.

Conclusion

Our study improves the understanding of the causal cascade of detailed physiological processes and structural responses related to tree water use and carbon sequestration using a tree-centered approach. Precise identification of the timing and severity of the physiological drought allowed us to demonstrate that the reduced capacity for wood formation (reflected in wood structure) induced a net loss of sequestrated carbon of 67% during a drought period in comparison to a regular year. This occurred despite attempts to mitigate drought stress by increasing the efficiency of water use and extending the duration of tracheid development. However, a resumption of the pre-drought growth rate upon release from the water deficit, through the use of previously unused assimilates, compensated for the growth impacts of the earlier drought stress.

Increments in size and in wall thickness are dissociated at the cellular level, and inconsistent bias could therefore occur when inferring tree carbon allocation without accounting for secondary wall deposition (Cuny *et al.*, 2015). This mismatch between xylem processes (enlargement and wall thickening) might partly explain discrepancies observed in studies that try to link ecosystem productivity with stem girth (Zweifel *et al.*, 2010) or tree-ring width series (Babst *et al.*, 2014). Our study provides novel insights into the mechanisms of responses that could support further development of sink model components of next generation DGVMs that include carbon sequestration based on wood processes (Zuidema *et al.*, 2018; Friend *et al.*, 2019b; Babst *et al.*, 2020; Eckes-Shephard *et al.*, 2021). Similar studies designed along ecological gradients and including more variability in impacting events would help to further test and calibrate such models.

ACKNOWLEDGEMENTS

We thank Lindsey Parkinson for help weighing in the isotope samples, Michael Matiu for providing NDVI data, Marina Fonti for preparing the slides for wood anatomical analyses, and Loic Schneider for support in lab logistics. Further, we acknowledge Lukas Emmenegger and his team, Béla Tuzson and Simone Pieber, for providing intra-annual atmospheric information on $\delta^{13}C$ and CO_2 concentrations from the Jungfraujoch research station (Davos, Switzerland), Carlos Herruzo Fonayet for help preparing Fig. S2, and Melissa Dawes for revising the manuscript. This study was funded by a WSL internal grant (project "Extremeimpact"), and by the Swiss National Science Foundation through projects TROXY (grant no. 175888; KT and EM-S:), LOTFOR (grant no. 150205; PF), and Ambizione TreeCarbo (grant no. 179978; MML).

AUTHOR CONTRIBUTIONS

EM-S and PF designed the study. EM-S performed the analysis and prepared the results. PF, KT, MML and AR contributed to the interpretation of the results. EM-S and PF led the writing, with many contributions from the other co-authors.

DATA AVAILABILITY

The data that support the findings of this study are available from the corresponding author upon reasonable request.

REFERENCES

Anderson-Teixeira KJ, Herrmann V, Rollinson CR, Gonzalez B, Gonzalez-Akre EB, Pederson N, Alexander MR, Allen CD, Alfaro-Sánchez R, Awada JL, *et al.* 2021. Joint effects of climate, tree size, and year on annual tree growth derived from tree-ring records of ten globally distributed forests. *Global Change Biology* **28**: 245-266.

Anderegg LDL, Anderegg WRL, Berry JA. 2013a. Not all droughts are created equal: Translating meteorological drought into woody plant mortality. *Tree Physiology* **33**: 701–712.

Anderegg WRL, Plavcová L, Anderegg LDL, Hacke UG, Berry J a, Field CB. 2013b. Drought's legacy: multiyear hydraulic deterioration underlies widespread aspen forest die-off and portends increased future risk. *Global Change Biology* **19**: 1188–96.

Anderegg WRL, Schwalm C, Biondi F, Camarero JJ, Koch G, Litvak M, Ogle K, Shaw JD, Shevliakova E, Williams AP, *et al.* 2015. Pervasive drought legacies in forest ecosystems and their implications for carbon cycle models. *Science* **349**: 528–532.

von Arx G, Carrer M. 2014. ROXAS – A new tool to build centuries-long tracheid-lumen chronologies in conifers. *Dendrochronologia* **32**: 290–293.

Babst F, Bouriaud O, Papale D, Gielen B, Janssens IA, Nikinmaa E, Ibrom A, Wu J, Bernhofer C, Köstner B, *et al.* 2014. Above-ground woody carbon sequestration measured from tree rings is coherent with net ecosystem productivity at five eddy-covariance sites. *New Phytologist* **201**: 1289–1303.

Babst F, Bouriaud O, Poulter B, Trouet V, Girardin MP, Frank DC. 2019. Twentieth century redistribution in climatic drivers of global tree growth. *Science Advances* **5**: eaat4313.

Babst F, Friend AD, Karamihalaki M, Wei J, von Arx G, Papale D, Peters RL. 2020. Modeling ambitions outpace observations of forest carbon allocation. *Trends in Plant Science* **26**: 1–10.

Babst F, Poulter B, Trouet V, Tan K, Neuwirth B, Wilson R, Carrer M, Grabner M, Tegel W, Levanic T, *et al.* 2013. Site- and species-specific responses of forest growth to climate across the European continent. *Global Ecology and Biogeography* **22**: 706–717.

Bala G, Caldeira K, Wickett M, Phillips TJ, Lobell DB, Delire C, Mirin A. 2007. Combined climate and carbon-cycle effects of large-scale deforestation. *Proceedings of the National Academy of Sciences of the United States of America* **104**: 6550–6555.

Balducci L, Cuny HE, Rathgeber CBK, Deslauriers A, Giovannelli A, Rossi S. 2016. Compensatory mechanisms mitigate the effect of warming and drought on wood formation. *Plant Cell and Environment* **39**: 1338–1352.

Battipaglia G, De Micco V, Brand WA, Saurer M, Aronne G, Linke P, Cherubini P. 2014. Drought impact on water use efficiency and intra-annual density fluctuations in *Erica arborea* on Elba (Italy). *Plant, Cell and Environment* **37**: 382–391.

Bennett AC, McDowell NG, Allen CD, Anderson-Teixeira KJ. 2015. Larger trees suffer most during drought in forests worldwide. *Nature Plants* **1**: 15139.

Betts RA, Boucher O, Collins M, Cox PM, Falloon PD, Gedney N, Hemming DL, Huntingford C, Jones CD, Sexton DMH, *et al.* 2007. Projected increase in continental runoff due to plant responses to increasing carbon dioxide. *Nature* **448**: 1037–1041.

Boettger T, Haupt M, Knöller K, Weise SM, Waterhouse JS, Rinne KT, Loader NJ, Sonninen E, Jungner H, Masson-Delmotte V, *et al.* 2007. Wood cellulose preparation methods and mass spectrometric analyses of $\delta^{13}C$, $\delta^{18}O$, and nonexchangeable $\delta^{2}H$ values in cellulose, sugar, and starch: An interlaboratory comparison. *Analytical Chemistry* **79**: 4603–4612.

Bögelein R, Lehmann MM, Thomas FM. 2019. Differences in carbon isotope leaf-to-phloem fractionation and mixing patterns along a vertical gradient in mature European beech and Douglas fir. *New Phytologist* **222**: 1803–1815.

Bonan GB. 2008. Forests and climate change: Forcings, feedbacks, and the climate benefits of forests. *Science* **320**: 1444–1449.

Bouche PS, Larter M, Domec JC, Burlett R, Gasson P, Jansen S, Delzon S. 2014. A broad survey of hydraulic and mechanical safety in the xylem of conifers. *Journal of Experimental Botany* **65**: 4419–4431.

Cabon A, Fernández-de-Uña L, Gea-Izquierdo G, Meinzer FC, Woodruff DR, Martínez-Vilalta J, De Cáceres M. 2020a. Water potential control of turgor-driven tracheid enlargement in Scots pine at its xeric distribution edge. *New Phytologist* **225**: 209–221.

Cabon A, Peters RL, Fonti P, Martínez-Vilalta J, De Cáceres M. 2020b. Temperature and water potential co-limit stem cambial activity along a steep elevational gradient. *New Phytologist* **226**: 1325–1340.

Camarero JJ, Gazol A, Sangüesa-Barreda G, Cantero A, Sánchez-Salguero R, Sánchez-Miranda A, Granda E, Serra-Maluquer X, Ibáñez R. 2018. Forest growth responses to drought at short- and long-term scales in Spain: Squeezing the stress memory from tree rings. *Frontiers in Ecology and Evolution* **6**: 1–11.

Camarero JJ, Olano JM, Parras A. 2010. Plastic bimodal xylogenesis in conifers from continental Mediterranean climates. *New Phytologist* **185**: 471–480.

Castagneri D, Battipaglia G, Von Arx G, Pacheco A, Carrer M. 2018. Tree-ring anatomy and carbon isotope ratio show both direct and legacy effects of climate on bimodal xylem formation in Pinus pinea. *Tree Physiology* **38**: 1098–1109.

Ciais P, Reichstein M, Viovy N, Granier A, Ogée J, Allard V, Aubinet M, Buchmann N, Bernhofer C, Carrara A, *et al.* 2005. Europe-wide reduction in primary productivity caused by the heat and drought in 2003. *Nature* **437**: 529–533.

Cuny HE, Fonti P, Rathgeber CBK, von Arx G, Peters RL, Frank DC. 2019. Couplings in cell differentiation kinetics mitigate air temperature influence on conifer wood anatomy. *Plant Cell and Environment* **42**: 1222–1232.

Cuny HE, Rathgeber CBK. 2016. Xylogenesis: Coniferous trees of temperate forests are listening to the climate tale during the growing season but only remember the last words! *Plant Physiology* **171**: 306–317.

Cuny HE, Rathgeber CBK, Frank D, Fonti P, Fournier M. 2014. Kinetics of tracheid development explain conifer tree-ring structure. *New Phytologist* **203**: 1231–1241.

Cuny HE, Rathgeber CBK, Frank D, Fonti P, Makinen H, Prislan P, Rossi S, Del Castillo EM, Campelo F, Vavrčík H, *et al.* 2015. Woody biomass production lags stem-girth increase by over one month in coniferous forests. *Nature Plants* **1**: 1–6.

Cuny HE, Rathgeber CBK, Kiessé TS, Hartmann FP, Barbeito I, Fournier M. 2013. Generalized additive models reveal the intrinsic complexity of wood formation dynamics. *Journal of Experimental Botany* **64**: 1983–1994.

Delpierre N, Lireux S, Hartig F, Camarero JJ, Cheaib A, Čufar K, Cuny H, Deslauriers A, Fonti P, Gričar J, *et al.* 2019. Chilling and forcing temperatures interact to predict the onset of wood formation in Northern Hemisphere conifers. *Global Change Biology* **25**:1089–1105.

Deslauriers A, Beaulieu M, Balducci L, Giovannelli A, Gagnon MJ, Rossi S. 2014. Impact of warming and drought on carbon balance related to wood formation in black spruce. *Annals of Botany* **114**: 335–345.

Dietrich L, Zweifel R, Kahmen A. 2018. Daily stem diameter variations can predict the canopy water status of mature temperate trees. *Tree Physiology* **38**: 941–952.
Dietze MC, Sala A, Carbone MS, Czimczik CI, Mantooth JA, Richardson AD, Vargas R. 2014. Nonstructural carbon in woody plants. *Annual Review of Plant Biology* **65**: 667–687.
Ditmarová L, Kurjak D, Palmroth S, Kmeť J, Střelcová K. 2009. Physiological responses of Norway spruce (*Picea abies*) seedlings to drought stress. *Tree Physiology* **30**: 205–213.
Eilmann B, Zweifel R, Buchmann N, Graf Pannatier E, Rigling A. 2011. Drought alters timing, quantity, and quality of wood formation in Scots pine. *Journal of Experimental Botany* **62**: 2763–71.
Etzold S, Sterck F, Bose AK, Braun S, Buchmann N, Eugster W, Gessler A, Kahmen A, Peters RL, Vitasse Y, *et al.* 2022. Number of growth days and not length of the growth period determines radial stem growth of temperate trees. *Ecology Letters* **25**: 427–439.
Farquhar GD, Ehleringer JR, Hubick KT. 1989. Carbon isotope discrimination and photosynthesis. *Annual Review of Plant Physiology and Plant Molecular Biology* **40**: 503–537.
Farquhar GD, Leary MHO, Berry JA. 1982. On the relationship between carbon isotope discrimination and the intercellular carbon dioxide concentration in leaves. *Australian Journal of Plant Physiology* **9**: 121–137.
Fatichi S, Luezinger S, Körner C. 2013. Moving beyond photosynthesis: from carbon source to sink-driven vegetation modeling. *New Phytologist* **201**: 1086–1095.
Fonti P, Heller O, Cherubini P, Rigling A, Arend M. 2013. Wood anatomical responses of oak saplings exposed to air warming and soil drought. *Plant Biology* **15**: 210–9.
Frank DC, Poulter B, Saurer M, Esper J, Huntingford C, Helle G, Treydte K, Zimmermann NE, Schleser GH, Ahlström A, *et al.* 2015. Water-use efficiency and transpiration across European forests during the Anthropocene. *Nature Climate Change* **5**: 579–583.
Friedlingstein P, Meinshausen M, Arora VK, Jones CD, Anav A, Liddicoat SK, Knutti R. 2014. Uncertainties in CMIP5 climate projections due to carbon cycle feedbacks. *Journal of Climate* **27**: 511–526.
Friedlingstein P, O'Sullivan M, Jones MW, Andrew RM, Hauck J, Olsen A, Peters GP, Peters W, Pongratz J, Sitch S, *et al.* 2020. Global Carbon Budget 2020. *Earth System Science Data* **12**: 3269–3340.
Friend AD, Eckes-Shephard AH, Fonti P, Rademacher TT, Rathgeber CBK, Richardson AD, Turton RH. 2019. On the need to consider wood formation processes in global vegetation models and a suggested approach. *Annals of Forest Science* **76**: 1-13.
Gao D, Joseph J, Werner RA, Brunner I, Zürcher A, Hug C, Wang A, Zhao C, Bai E, Meusburger K, *et al.* 2021. Drought alters the carbon footprint of trees in soils—tracking the spatio-temporal fate of ^{13}C-labelled assimilates in the soil of an old-growth pine forest. *Global Change Biology* **27**: 2491–2506.
Génard M, Fishman S, Vercambre G, Huguet JG, Bussi C, Besset J, Habib R. 2001. A biophysical analysis of stem and root diameter variations in woody plants. *Plant Physiology* **126**: 188–202.
Gessler A, Bottero A, Marshall J, Arend M. 2020. The way back: recovery of trees from drought and its implication for acclimation. *New Phytologist* **228**: 1704–1709.
Gessler A, Ferrio JP, Hommel R, Treydte K, Werner RA, Monson RK. 2014. Stable isotopes in tree rings: Towards a mechanistic understanding of isotope fractionation and mixing processes from the leaves to the wood. *Tree Physiology* **34**: 796–818.
Hacke UG, Jansen S. 2009. Embolism resistance of three boreal conifer species varies with pit structure. *New Phytologist* **182**: 675–686.
Hagedorn F, Joseph J, Peter M, Luster J, Pritsch K, Geppert U, Kerner R, Molinier V, Egli S, Schaub M, *et al.* 2016. Recovery of trees from drought depends on belowground sink control. *Nature Plants* **2**:1-5.
Harris NL, Gibbs DA, Baccini A, Birdsey RA, de Bruien S, Farina M, Fatoyinbo L, Hansen MC, Herold M, Houghton RA, *et al.* 2021. Global maps of twenty-first century forest carbon fluxes. *Nature Climate Change* **11**: 234–240.

Hilty J, Muller B, Pantin F, Leuzinger S. 2021. Plant growth: the What, the How, and the Why. *New Phytologist* **232**: 25–41.

Hsiao TC. 1973. Plant responses to water stress. *Annual Review of Plant Physiology* **24**: 519–570.

Huang J.-G, Ma Q, Rossi S, Biondi F, Deslauriers A, Fonti P, Liang E, Mäkinen H, Oberhuber W, Rathgeber CBK, *et al*. 2020. Photoperiod and temperature as dominant environmental drivers triggering secondary growth resumption in Northern Hemisphere conifers. *Proceedings of the National Academy of Sciences* **117**:20645–20652.

IPCC. 2021. *Climate Change 2021: The Physical Science Basis. Working Group I contribution to Sixth Assessment Report of the Intergovernmental Planel on Climate Change*.

Kagawa A, Sugimoto A, Yamashita K, Abe H. 2005. Temporal photosynthetic carbon isotope signatures revealed in a tree ring through $^{13}CO_2$ pulse-labelling. *Plant, Cell and Environment* **28**: 906–915.

Klein T. 2014. The variability of stomatal sensitivity to leaf water potential across tree species indicates a continuum between isohydric and anisohydric behaviours. *Functional Ecology* **28**: 1313–1320.

Klesse S, Babst F, Lienert S, Spahni R, Joos F, Bouriaud O, Carrer M, Di Filippo A, Poulter B, Trotsiuk V, *et al.* 2018. A combined tree ring and vegetation model assessment of European forest growth sensitivity to interannual climate variability. *Global Biogeochemical Cycles* **32**: 1226–1240.

Körner C. 2015. Paradigm shift in plant growth control. *Current Opinion in Plant Biology* **25**: 107–114.

Lachenbruch B, Mcculloh KA. 2014. Traits, properties, and performance: How woody plants combine hydraulic and mechanical functions in a cell, tissue, or whole plant. *New Phytologist* **204**: 747–764.

Laumer W, Andreu L, Helle G, Schleser GH, Wieloch T, Wissel H. 2009. A novel approach for the homogenization of cellulose to use micro-amounts for stable isotope analyses. *Rapid Communications in Mass Spectrometry* **23**: 1934–1940.

Lebourgeois F, Rathgeber CBK, Ulrich E. 2010. Sensitivity of French temperate coniferous forests to climate variability and extreme events (*Abies alba*, *Picea abies* and *Pinus sylvestris*). *Journal of Vegetation Science* **21**: 364–376.

Lovenduski NS, Bonan GB. 2017. Reducing uncertainty in projections of terrestrial carbon uptake. *Environmental Research Letters* **12**: 044020.

Lu P, Biron P, Bréda N, Granier A. 1995. Water relations of adult Norway spruce (*Picea abies* (L) Karst) under soil drought in the Vosges mountains: water potential, stomatal conductance and transpiration. *Annales des Sciences Forestieres* **52**: 117–129.

Martin-Benito D, Beeckman H, Cañellas I. 2013. Influence of drought on tree rings and tracheid features of *Pinus nigra* and *Pinus sylvestris* in a mesic Mediterranean forest. *European Journal of Forest Research* **132**: 33–45.

Olano JM, Linares JC, García-Cervigón AI, Arzac A, Delgado A, Rozas V. 2014. Drought-induced increase in water-use efficiency reduces secondary tree growth and tracheid wall thickness in a Mediterranean conifer. *Oecologia* **176**: 273–283.

Orth R, Zscheischler J, Seneviratne SI. 2016. Record dry summer in 2015 challenges precipitation projections in Central Europe. *Scientific Reports* **6**: 1–8.

Pan Y, Birdsey R, Fang J, Houghton R, Kauppo PE, Kurz WA, Phillips OL, Shvidenko A, Lewis SL, Canadell JG, *et al.* 2011. A large and persistent carbon sink in the World's forests. *Science* **333**: 988–993.

Pérez-de-Lis G, Rathgeber CBK, Fernández-de-Uña L, Ponton S. 2021. Cutting tree rings into time slices: How intra-annual dynamics of wood formation help decipher the space-for-time conversion. *New Phytologist* **233**: 1520–1534.

Peters RL, Balanzategui D, Hurley AG, von Arx G, Prendin AL, Cuny HE, Björklund J, Frank DC, Fonti P. 2018. RAPTOR: Row and position tracheid organizer in R. *Dendrochronologia* **47**: 10–16.

Peters RL, Steppe K, Cuny HE, De Pauw DJW, Frank DC, Schaub M, Rathgeber CBK, Cabon A, Fonti P. 2020. Turgor – a limiting factor for radial growth in mature conifers along an elevational gradient. *New Phytologist* **229**: 213-229.

Piper FI, Fajardo A, Hoch G. 2017. Single-provenance mature conifers show higher non-structural carbohydrate storage and reduced growth in a drier location. *Tree Physiology* **37**: 1001–1010.

R Development Core Team. 2015. A Language and Environment for Statistical Computing. R Foundation for Statistical Computing, Vienna, Austria. URL http://www.R-project.org/.

Rademacher T, Fonti P, LeMoine JM, Fonti M V., Basler D, Chen Y, Friend AD, Seyednasrollah B, Eckes-Shephard AH, Richardson AD. 2021. Manipulating phloem transport affects wood formation but not local nonstructural carbon reserves in an evergreen conifer. *Plant Cell and Environment* **44**: 2506–2521.

Rathgeber CBK, Cuny HE, Fonti P. 2016. Biological basis of tree-ring formation: A crash course. *Frontiers in Plant Science* **7**: 1–7.

Raven JA. 2002. Selection pressures on stomatal evolution. *New Phytologist* **153**: 371–386.

Reichstein M, Bahn M, Ciais P, Frank D, Mahecha MD, Seneviratne SI, Zscheischler J, Beer C, Buchmann N, Frank DC, *et al.* 2013. Climate extremes and the carbon cycle. *Nature* **500**: 287–295.

Rossi S, Anfodillo T, Menardi R. 2006a. Trephor: A new tool for sampling microcores from tree stems. *IAWA Journal* **27**: 89–97.

Rossi S, Deslauriers A, Anfodillo T. 2006b. Assessment of cambial activity and xylogenesis by microsampling tree species: an example at the alpine timberline. *IAWA Journal* **27**: 383–394.

Rossi S, Deslauriers A, Griçar J, Seo J.-W, Rathgeber CB, Anfodillo T, Morin H, Levanic T, Oven P, Jalkanen R. 2008. Critical temperatures for xylogenesis in conifers of cold climates. *Global Ecology and Biogeography* **17**:696–707.

Rossi S, Girard MJ, Morin H. 2014. Lengthening of the duration of xylogenesis engenders disproportionate increases in xylem production. *Global Change Biology* **20**: 2261–2271.

Salomón RL, Peters RL, Zweifel R, Sass-Klaassen UGW, Stegehuis AI, Smiljanic M, Poyatos R, Babst F, Cienciala E, Fonti P, *et al.* 2022. The 2018 European heatwave led to stem dehydration but not to consistent growth reductions in forests. *Nature Communications* **13**: 1–11.

Sarris D, Siegwolf R, Körner C. 2013. Inter- and intra-annual stable carbon and oxygen isotope signals in response to drought in Mediterranean pines. *Agricultural and Forest Meteorology* **168**: 59–68.

Sass-Klaassen U, Fonti P, Cherubini P, Gričar J, Robert EMR, Steppe K, Bräuning A. 2016. A tree-centered approach to assess impacts of extreme climatic events on forests. *Frontiers in Plant Science* **7**: 1–6.

Schäfer C, Rötzer T, Thurm EA, Biber P, Kallenbach C, Pretzsch H. 2019. Growth and tree water deficit of mixed Norway spruce and European beech at different heights in a tree and under heavy drought. *Forests* **10**: 577.

Schlesinger WH, Jasechko S. 2014. Transpiration in the global water cycle. *Agricultural and Forest Meteorology* **189–190**: 115–117.

Shestakova TA, Martínez-Sancho E. 2021. Stories hidden in tree rings: a review on the application of stable carbon isotopes to dendrosciences. *Dendrochronologia* **65**: 125789.

Slette IJ, Post AK, Awad M, Even T, Punzalan A, Williams S, Smith MD, Knapp AK. 2019. How ecologists define drought, and why we should do better. *Global Change Biology* **25**: 3193–3200.

Stangler DF, Kahle HP, Raden M, Larysch E, Seifert T, Spiecker H. 2021. Effects of intra-seasonal drought on kinetics of tracheid differentiation and seasonal growth dynamics of norway spruce along an elevational gradient. *Forests* **12**: 1–27.

Sviderskaya I V., Vaganov EA, Fonti M V., Fonti P. 2021. Isometric scaling to model water transport in conifer tree rings across time and environments. *Journal of Experimental Botany* **72**: 2672–2685.

Timofeeva G, Treydte K, Bugmann H, Rigling A, Schaub M, Siegwolf R, Saurer M. **2017**. Long-term effects of drought on tree-ring growth and carbon isotope variability in Scots pine in a dry environment. *Tree Physiology* **37**: 1028–1041.

Tomasella M, Häberle KH, Nardini A, Hesse B, Machlet A, Matyssek R. 2017. Post-drought hydraulic recovery is accompanied by non-structural carbohydrate depletion in the stem wood of Norway spruce saplings. *Scientific Reports* **7**: 1-13.

Trotsiuk V, Hartig F, Cailleret M, Babst F, Forrester DI, Baltensweiler A, Buchmann N, Bugmann H, Gessler A, Gharun M, *et al.* 2020. Assessing the response of forest productivity to climate extremes in Switzerland using model–data fusion. *Global Change Biology* **26**: 2463–2476.

Walker AP, De Kauwe MG, Bastos A, Belmecheri S, Georgiou K, Keeling RF, McMahon SM, Medlyn BE, Moore DJP, Norby RJ, *et al.* 2020. Integrating the evidence for a terrestrial carbon sink caused by increasing atmospheric CO_2. *New Phytologist*: 2413–2445.

Werner C, Meredith LK, Nemiah Ladd S, Ingrisch J, Kübert A, van Haren J, Bahn M, Bailey K, Bamberger I, Beyer M, *et al.* *Ecosystem fluxes during drought and recovery in an experimental forest*. *Science* **374**: 1514-1518.

Wickham H. **2009**. ggplot2: Elegant Graphics for Data Analysis. R package version 3.3.5.

Wood S. **2006**. *Generalized Additive Models: An Introduction with R*. Boca Raton, FL. Chapman and Hall/CRC.

Xu L, Saatchi SS, Yang Y, Yu Y, Pongratz J, Bloom AA, Bowman K, Worden J, Liu J, Yin Y, *et al.* 2021. Changes in global terrestrial live biomass over the 21st century. *Science Advances*, **7**: eabe9829.

Zang CS, Buras A, Esquivel-Muelbert A, Jump AS, Rigling A, Rammig A. **2020**. Standardized drought indices in ecological research: Why one size does not fit all. *Global Change Biology* **26**: 322–324.

Zuidema PA, Poulter B, Frank DC. **2018**. A wood biology agenda to support global vegetation modelling. *Trends in Plant Science* **23**: 1006–1015.

Zweifel R, Eugster W, Etzold S, Dobbertin M, Buchmann N, Häsler R. **2010**. Link between continuous stem radius changes and net ecosystem productivity of a subalpine Norway spruce forest in the Swiss Alps. *New Phytologist* **187**: 819–830.

Zweifel R, Haeni M, Buchmann N, Eugster W. **2016**. Are trees able to grow in periods of stem shrinkage? *New Phytologist* **211**: 839–849.

Zweifel R, Zimmermann L, Newbery DM. **2005**. Modeling tree water deficit from microclimate: an approach to quantifying drought stress. *Tree Physiology* **25**: 147–156.

TABLES

Table 1. Critical dates for each phase of wood formation of Norway spruce, expressed as mean day of year.

	2014	2015
bE	138 ± 1.7	138.3 ± 6.4
bW	155 ± 2.9	158 ± 0.0
bM	165 ± 10.5	162 ± 3.8
cE	**260 ± 2.9**	**251 ± 4.3**
cW	285 ± 3.5	290 ± 5.0
dE	121 ± 2.2	113 ± 9.0
dW	130 ± 4.6	131 ± 5.0
dX	147 ± 1.9	151 ± 7.4

bE, beginning of the cell enlargement phase; bW, beginning of the cell wall thickening phase; bM, beginning of the mature cell phase; cE, cessation of the cell enlargement phase; cW, cessation of the cell wall thickening phase; dE, duration of the cell enlargement phase; dW, duration of the cell wall thickening phase; dX, total duration of wood formation. A t-test was performed to assess differences between the two years; bold values indicate significant differences (P <0.05).

FIGURES

Figure 1. Environmental and physiological conditions during the 2014 (normal) and 2015 (dry) growing seasons. (A) Maximum daytime air temperature (T AIR), average daytime relative humidity (RH), average daytime vapor pressure deficit (VPD), and soil volumetric water content (SVWC). (B) Normalized difference vegetation index (NVDI). Dots represent four-day composite NDVI values. (C) Daily dendrometer-derived tree water deficit (TWD), measured as a negative change in stem radius.

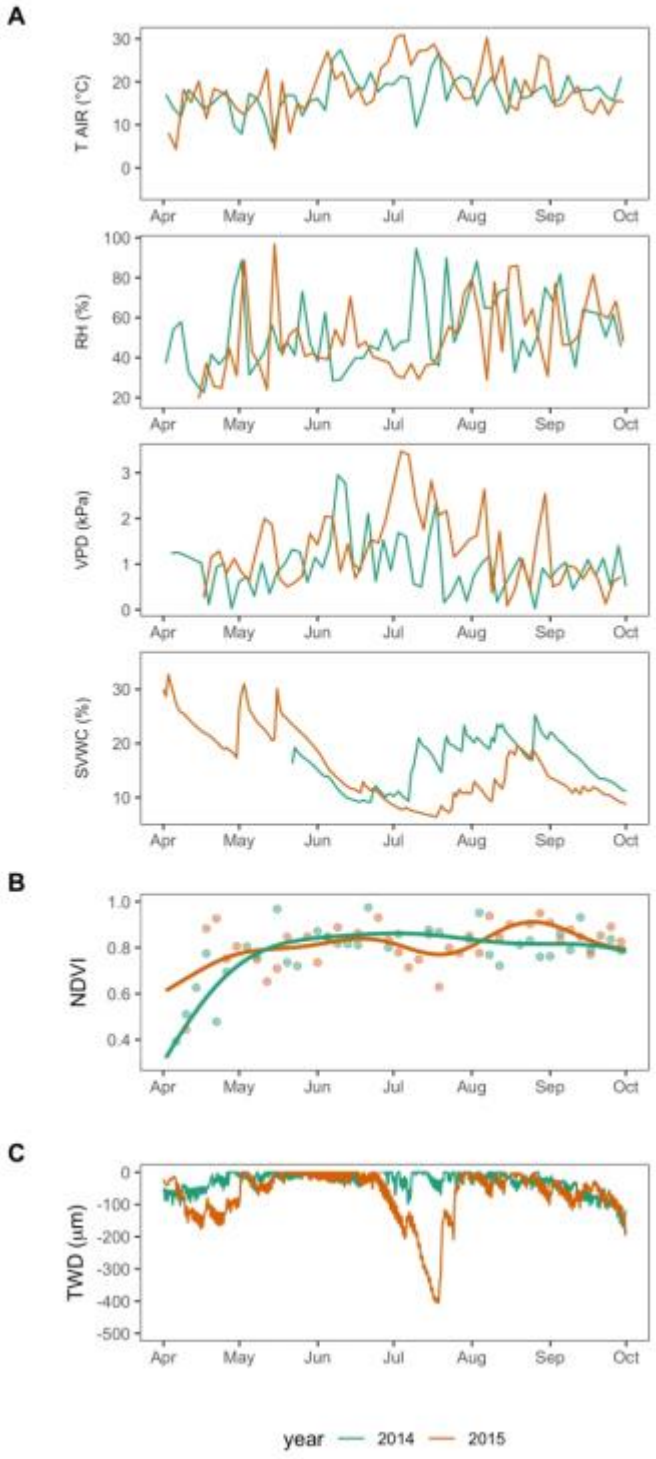
A
T AIR (°C)
RH (%)
VPD (kPa)
SVWC (%)
Apr
May
Jun
Jul
Aug
Sep
Oct
B
NDVI
C
TWD (µm)
year
2014
2015

Figure 2. Comparison of the number of cells in the cambial, enlargement, wall thickening and mature phases in the two study years for the four studied Norway spruce trees. Colored lines indicate the fitted values obtained from generalized additive mixed models and the corresponding shaded colored areas indicate the 95% confidence intervals. The grey band indicates the period when the tree water deficit (TWD; negative change in stem radius in μm) for more than 24 h during the extreme summer drought in 2015.

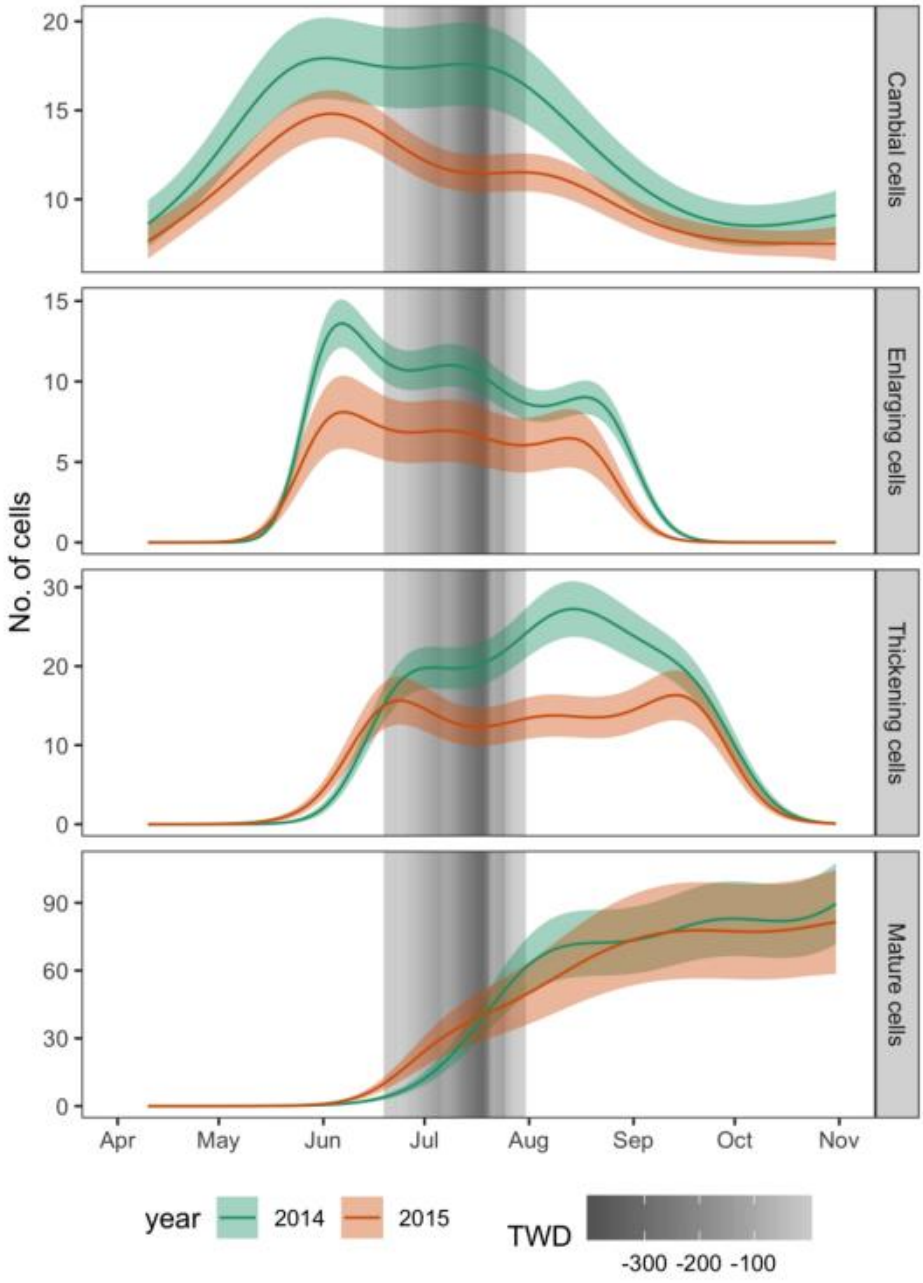

Figure 3. Anatomical features (cell area, cell wall area and cell lumen area) and rates of cell differentiation in the years 2014 and 2015 for the four studied Norway spruce trees. The anatomical features are aligned by position within the ring width (A, D, G) and by time of cell formation (B, E, H). Differences in rates of cell enlargement and wall thickening are also displayed (C, F), where each rectangle represents a single modelled cell. Colored lines (A, C, D, F, G) indicate the fitted values obtained from generalized additive mixed models and the corresponding shaded colored areas indicate the 95% confidence intervals. The grey band (B, C, E, F, H) indicates the period when the tree water deficit (TWD; negative change in stem radius in μm) for more than 24 h during the extreme summer drought in 2015.

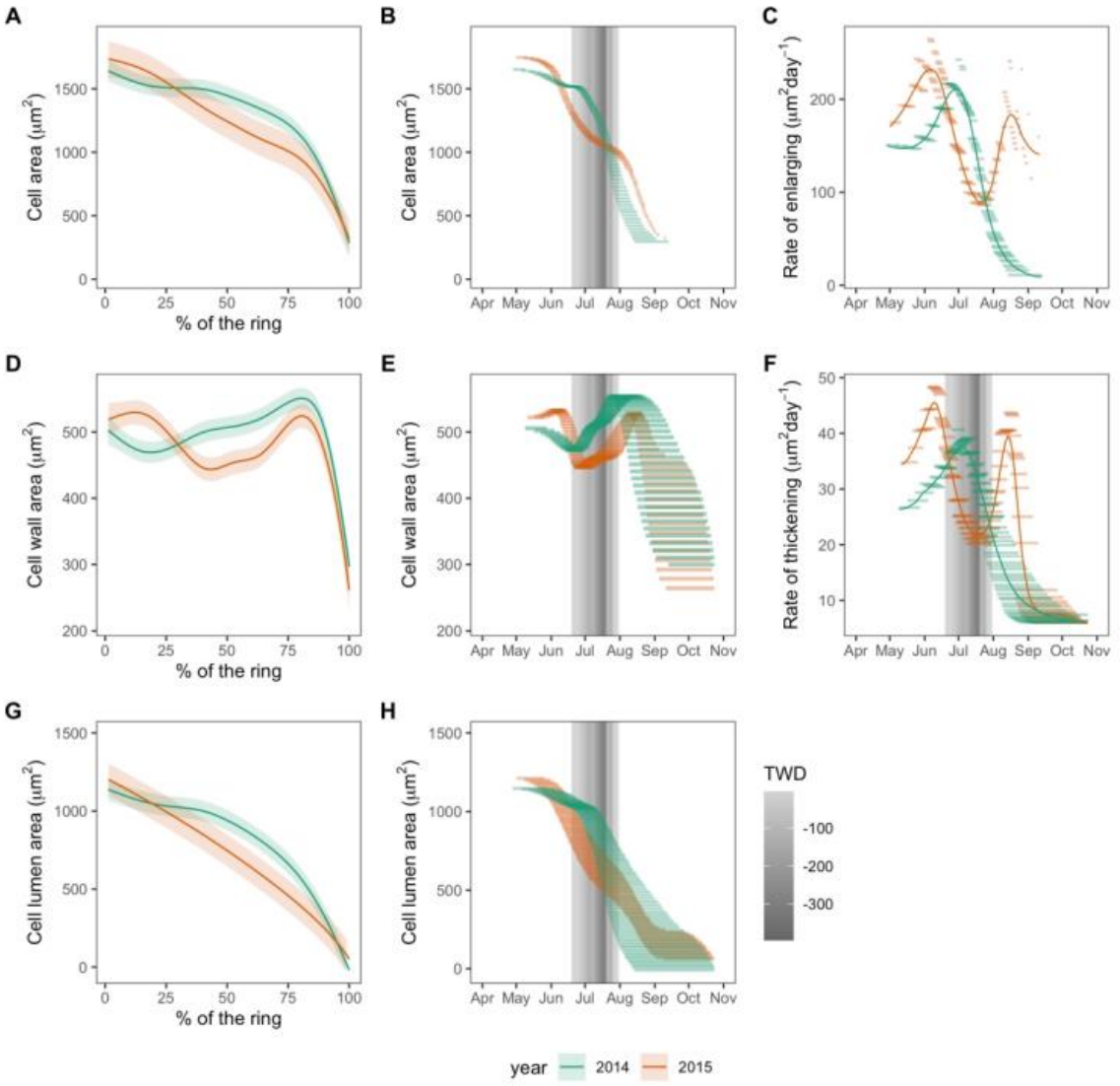

Figure 4. Intra-annual tree-ring cellulose $\delta^{13}C$ patterns for 2014 and 2015 and derived parameters aligned by ring position (A) and time of cell wall formation (B, C, D, E) for the four studied Norway spruce trees. In (B, C, D, E), each rectangle represents a single modelled cell. $\Delta^{13}C$, discrimination against ^{13}C; Ci, leaf intercellular CO_2 concentration; and iWUE, intrinsic water-use efficiency. In (A), the colored lines indicate the fitted values obtained from generalized additive mixed models and the corresponding shaded colored areas indicate the 95% confidence intervals. The grey band indicates the period when the tree water deficit (TWD; negative change in stem radius in μm) was negative for more than 24 h during the extreme summer drought in 2015.

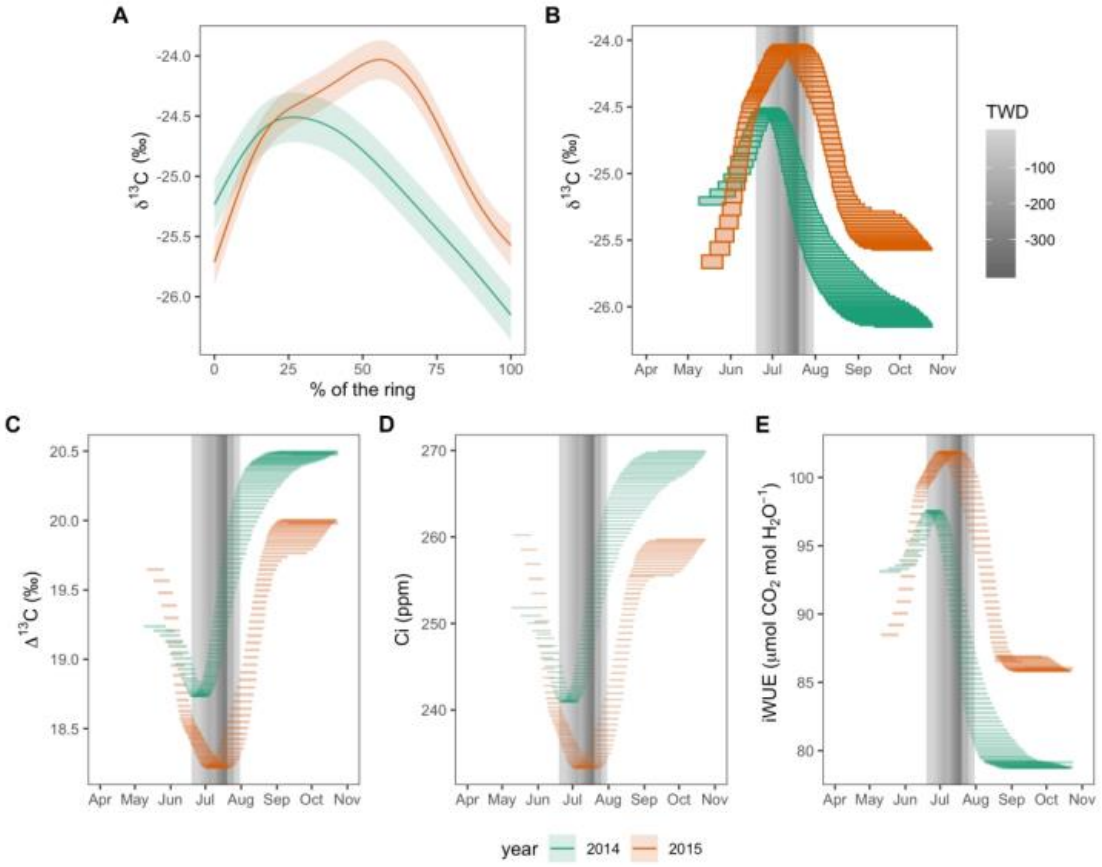

Figure 5. Seasonal dynamics of daily carbon sequestration of Norway spruce in 2014 and 2015. The tree carbon gain is represented by carbon in woody biomass production and was calculated based on daily wall thickness increments. The grey band indicates the period when the tree water deficit (TWD; negative change in stem radius in μm) was negative for more than 24 h during the extreme summer drought in 2015.

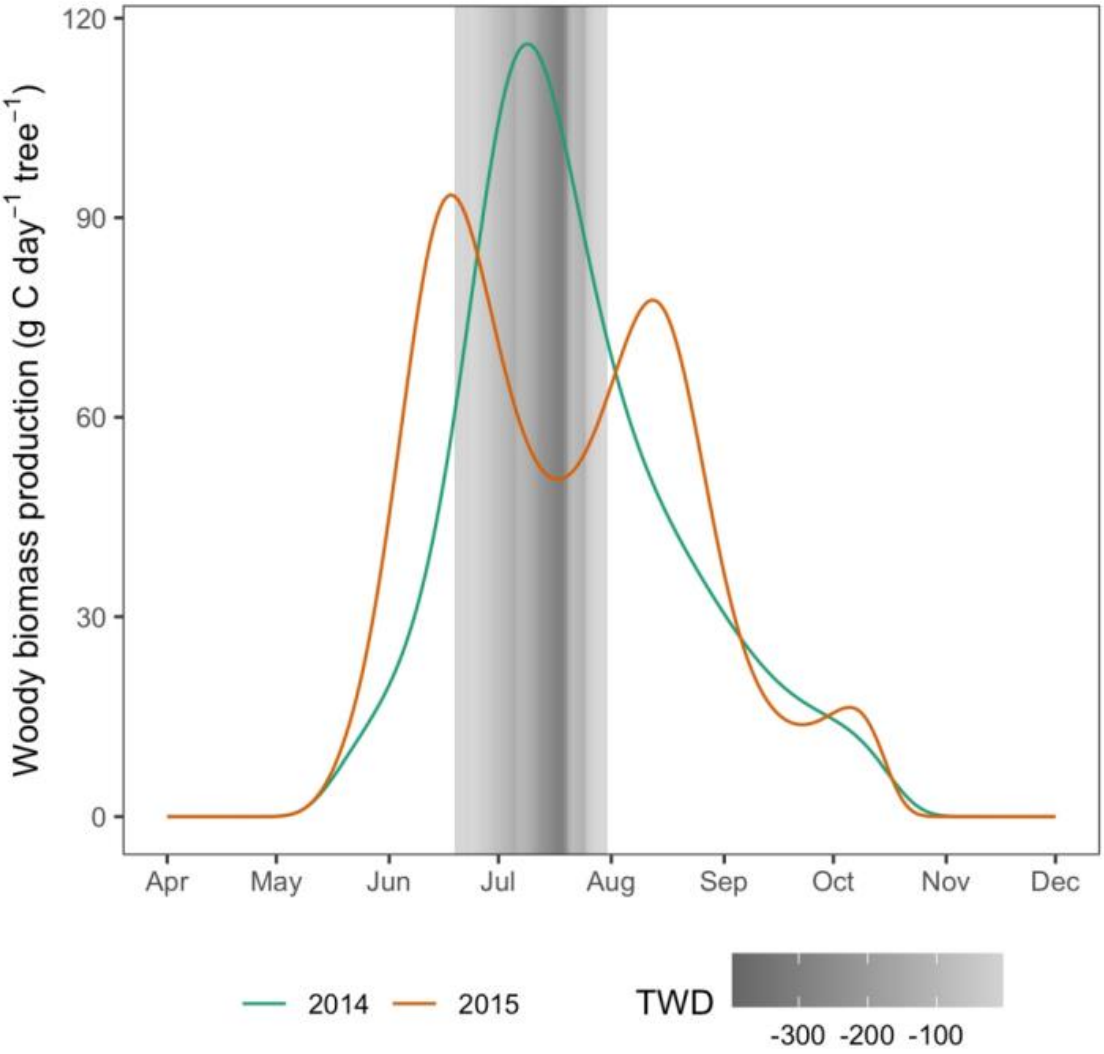

Supporting information